On the Aerodynamics of Rear of Vehicle Model with Active Control by Blowing: Computational and Experimental Analysis

Rustan Tarakka [1]*, Nasaruddin Salam [1], Andi Amijoyo Mochtar [1], Wawan Rauf [2], Muhammad Ihsan [3]

[1] Department of Mechanical Engineering, Hasanuddin University, Gowa, Indonesia;
Email:{nassalam.unhas@yahoo.co.id}{andijoyo@unhas.ac.id}
[2] Department of Mechanical Engineering, Gorontalo University, Gorontalo, Indonesia; Email:
{wawanrauf241193@yahoo.com }
[3] Department of Civil Engineering, Sekolah Tinggi Teknik Baramuli, Pinrang, Indonesia; Email:
{muhammadihsan@alumni.ait.asia}
*Correspondence: rustan_tarakka@yahoo.com

Abstract—**Aerodynamics related to the generation of drag due to flow separations that occurs at rear parts of vehicles is an important consideration in vehicle design. It includes flow separation, wake formation, and pressures, which, in this paper, are focused on the ones exerted on the model's rear wall. The pressure reductions could differ significantly between vehicles' front and rear walls. This pressure difference can generate a phenomenon of backward pull and an increase in drags. The effort to minimize backflow as well as to cater increasing pressure on vehicles' rear wall can be achieved by applying active control, including attached blowing apparatus. The paper presents the analysis of the effect on the application of blowing active control on the aerodynamics on rear part of vehicles, which is represented by a modified Ahmed body, reversed in flow direction and altered dimensions. The research was conducted using a validated numerical simulation method with laboratory experiments at an upstream air speed of 16.7 m/s and blowing velocities of 0.5 m/s, 1.0 m/s, and 1.5 m/s. The results showed that the application of blowing active control was capable to reduce aerodynamic drag, with the highest decrease achieved in the model with a ratio of velocity UBL3/U0=0.09 of 12.187% for the computational method and 11.556% for the experimental one.**

Keywords—**aerodynamic drag, blowing active control, vehicle model**

I. INTRODUCTION

Aerodynamics related to the generation of drag due to flow separations at rear parts of vehicles is an important consideration in vehicle design. The magnitude of the aerodynamic drag force, works in contrast to the relative motion of a moving object, undergone by vehicles will affect vehicles' energy consumption and stability [1, 2]. This opposing movement usually occurs between the fluid and the surface of a solid object [3]. One approximation on amount of fuel consumption to overcome these adverse

aerodynamic drag is about 50-60% [4]. Reduction of the aerodynamic drag by as small as 15% will contribute to 5-7% fuel consumption savings [5].

The aerodynamic drag on a vehicle is closely related to the flow characteristics and the pressure distribution at the rear part, which are also influenced by flow separations occurring at the upper rear part [6]. The design of this part is then very important in the effort of reducing aerodynamic drag [7]. The flow separation is expected to cause backflow and decrease pressure field in the onset area of the separation. The rate of the flow separation tends to increase the extent of the wake area positively and, at the same time, reduce the pressure on the rear wall region. This results in notable differences in the pressure exerted at both front and rear parts, triggering the backward pull phenomenon [8]. The process of minimizing negative pressure, and the intensity, at the rear area of vehicles could decrease the aerodynamic drag [4].

Flow engineering is a method used to minimize backflow and, at the same time, increase pressures exerted on the rear parts. As a results, it positively impacts delaying separation and reducing the re-circulation zone. Furthermore, flow engineering is realized by the application of active controls, such as blowing, with a combination with other forms of control, either active or passive [7], [9], [10].

An investigation carried out on the effect of continuous blowing on the interface of vehicles' roof and rear window was published by Mestiri et al. Based on an experiment performed on steady blowing at 25 °tangent to the surface of the slanted rear window of an Ahmed model, it was proven that tangential steady blowing produced the separated area on the rear window as well as disturbed the appearance of the counter-rotating longitudinal vortex at the end side. Furthermore, the direct flow control was considered effective in the re-circulation area at the upper part of the rear window [11].

A study has been carried out on the potentials of aerodynamic drag reductions of a city-car prototype (a baseline version of the XAM 2.0). It employed air blow and relief flow control devices embedded into the vehicle's wheel, in a dedicated wind tunnel, with special arrangement to reduce turbulences at the front wheel, and to cope with the air-flow disturbance at the end of vehicles' side body. The study further incorporated a CFD analysis to evaluate the effects of the modifications. By validating the drag optimization, a correlation of experimental results by wind tunnel results and the CFD results was obtained, showing anticipated capabilities of CFD analysis, as well as a record-breaking outcome in drag coefficients [12].

Tebbiche and Boutoudj have recently published an experimental investigation carried out to determine the effect of the various blowing rates and Reynolds numbers for some incidences of airfoils, two angles of Ahmed body's rear windows, and a set of flow velocities (15-30 m/s) in a subsonic wind tunnel. The results showed improvements in the aerodynamic coefficients. For example, on a $20°$ tilted rear window of Ahmed body model, 3.6% drag reduction was confirmed due to the application of a minimum blowing intensity $C\mu = 0.28\%$. A notable 15% reduction was gained by maximum $C\mu = 4.79\%$. Additionally, a high-drag regime related to a $30°$ tilted rear window produced a drag reduction of 19% at $C\mu = 5\%$ [13].

Cerutti et al. conducted an experimental research on the manipulation of the generation of on a square-back model by four rectangular jets blowing continuously by means of standart and stereoscopic Particle Image Velocimetry (PIV and sPIV), and revealed a considerable alteration in the maximum drag reduction on the formation of wake as the jets blow, while similar wake structure was best compromised [14].

II. METHOD

The present research focuses on the modified Ahmed body, altered in the orientation of the flow and the dimensional ratio to the original Ahmed body, set at 0.17 (1:6). The dimensions are 174 mm length (l), 48 mm height (l), and 64.83 mm width (w), with $35°$ slant angle of the model's front geometry. The upper rear side of the vehicle model is designated as the area where the blowing active control is located. The active controls present in 5 slots with a diameter of 7 mm and a distance of 10.81 mm between apertures. Each circle is defined as B_{L1}, B_{L2}, B_{L3}, B_{L4}, and B_{L5}. The tests were carried out by setting the blowing velocity of each apertures (BL), $U_{BL1}=0.5$ m/s, $U_{BL2}=1.0$ m/s, and $U_{BL3}=1.5$ m/s at the upstream speed of $U_0=16.7$ m/s. The ratios of blowing velocity to upstream velocity are stated as follows $U_{BL1}/U_0=0.03$, $U_{BL2}/U_0=0.06$, and $U_{BL3}/U_0=0.09$. Furthermore, a detailed model setup is shown in Fig. 1.
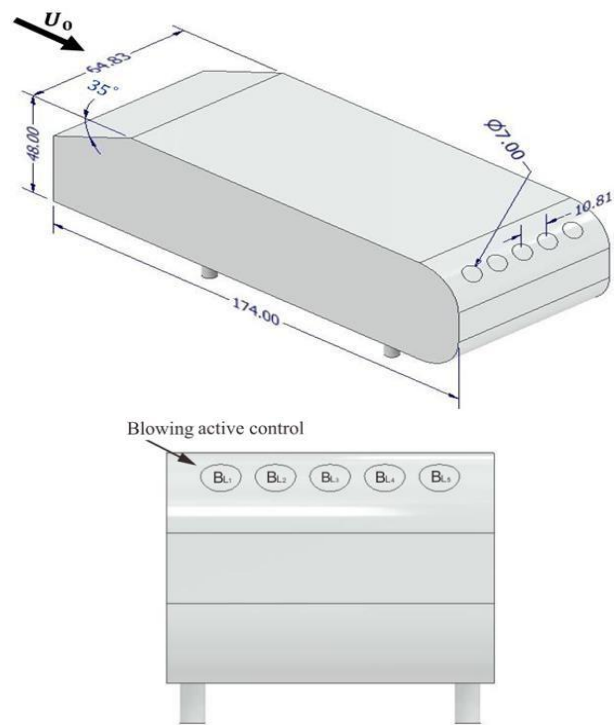
Figure 1. Test model.

This research covers the flow characteristics passing through the model's rear, the pressure field (C_p), and aerodynamic drag (C_d). The aerodynamic drag (C_d) is investigated by computational and by experimental observations. For flow characteristics and pressure field (C_p), the investigations were based only on numerical simulation using a standard k—epsilon turbulence model with tetrahedral meshing. The definition of turbulence model and meshing type is based on previous work of Harinaldi *et al.* [15]. The data collection on pressure distribution have been conducted at model's rear parts, considering the location is prone to the separation of flow and wake to generate, resulting negative pressures contributing up to 80% of the total drag [16]. On the models' transversal axis, the information on pressure are obtained from five different grid lines, where grid-to-model width ratios are defined as z/w=-0.5, z/w=-0.25, z/w=0, z/w=0.25, and z/w=0.5. With respect to model height axis, pressure data have been obtained from five grid lines for models without control and four for those with blowing active controls. The grid-to-model height ratios l (y/h) are as follows 0.17, 0.33, 0.50, 0.67, and 0.83. The pressure field data collection area are shown in Fig. 2 and are incorporated into the pressure coefficient (C_p) value obtained using Eq. (1) [17].

$$C_p = \frac{(P - P_0)}{\frac{1}{2}\rho v^2} \tag{1}$$

(a)

(b)
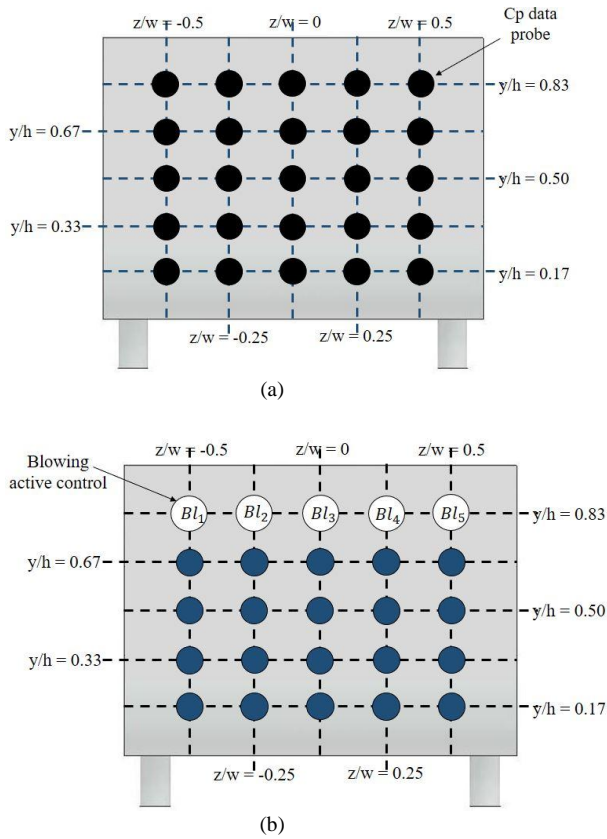
Figure 2. Cp data probe: (a) without control, (b) with blowing active control

Figure 3. Computational domain.
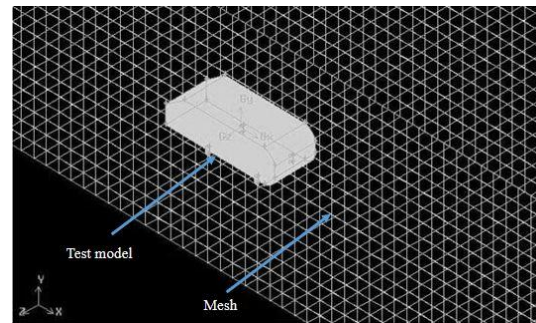
Figure 4. Computational mesh.

The simulation utilized Fluent 6.3.26 ANSYS computational fluid dynamic software. Additionally, the vehicle model is designed using Autodesk Inventor™. Fig. 3 and Table I depict the computational domain, while Fig. 4 presents the meshing process in Gambit™ software.

TABLE I. COMPUTATIONAL CONDITIONS

Boundary condition	Type	Value
Fluid properties	Density	1.225 kg/m^3
	Viscosity	1.7894 $\times 10^{-5}$
Model boundary conditions without control	Model	Wall
	Outlet	Pressure outlet
	Inlet	Velocity inlet
		Wall
Boundary conditions of the model with blowing active controls	Model	Wall
	Outlet	Pressure outlet
	Inlet	Velocity inlet
	Wall	Wall
	U_{BL1} U_{BL2}, U_{BL3}, U_{BL4}, U_{BL5}	Velocity inlet

The experimental testing has utilized the sub-sonic wind tunnel facility. The measurement of drag used a load cell equipped with an Arduino device directly connected to a computer. The duration of data retrieval is 120 seconds, generating 120 data for each velocity ($U_{BL1}/U_0=0.03$, $U_{BL2}/U_0=0.06$, and $U_{BL3}/U_0=0.09$). This information is then averaged to gain drag values for each velocity comparison with high accuracy. The schematic of experimental setup is depicted in Fig. 5.
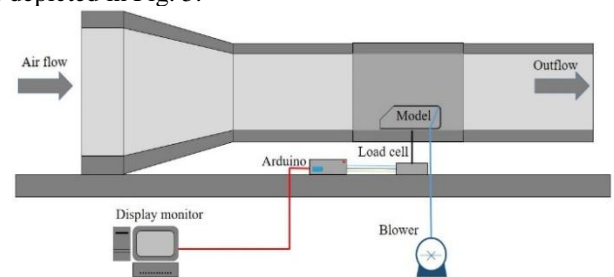
Figure 5. Experimental setup.

The drag force is transformed a into non-dimensional drag coefficient (C_d) by using Eq. (2) [18]:

$$C_d = \frac{F_d}{\frac{1}{2}\rho v^2 A} \qquad (2)$$

III. RESULTS AND DISCUSSION

A. Flow Field

The characteristics of the flow pattern of the test model with active control in the ratio of blowing velocity to upstream velocity, $U_{BL1}/U_0=0.03$, $U_{BL2}/U_0=0.06$ and $U_{BL3}/U_0=0.09$ as well as those without control are shown in Fig. 6. The model without active control shows a large

wake structure caused by the flow separation on the upper rear side as shown in Fig. 6(a). The air flow, which initially flowed uniformly, later formed backflow and re-circulation areas. This is the main cause of negative pressure, which leads to the phenomenon of backward pulling. The re-atraction process has been suspected as a major contributor to the extent of aerodynamic drag, besides other presumed factor of longitudinal vortex [19]. Visually, the model without active control has a fairly large longitudinal vortex structure. This is because the fluid loses its momentum to move along the rear body due to the friction force, thereby resulting in differences in flow velocities on the rear side and the center of the vehicles. This varying speed forces the flow on the middle side to flow sidebound to form a longitudinal vortex.

For models with the blowing at the velocity ratio, $U_{BL1}/U_0=0.03$, $U_{BL2}/U_0=0.06$ and $U_{BL3}/U_0=0.09$, as presented in Figs. 6(b), 6(c) and 6(d), the wake structure is smaller than the one on the model without application of control. This is because there is a delay in flow separation, where the separation process is formed in an area far from the rear wall of the model, and minimize the intensity of the backflow interacting with the rear wall. The longitudinal vortex formed tends to be smaller due to the blowing effect which forces a portion of the flow on the upper wall to move straight toward the downstream area. The model in the velocity ratio $U_{BL3}/U_0=0.09$ shows smaller wake formation compared to those at the velocity rations $U_{BL1}/U_0=0.03$ and $U_{BL2}/U_0=0.06$.
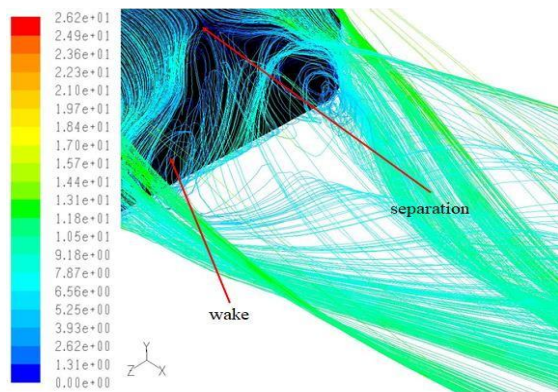
(a)   Without control
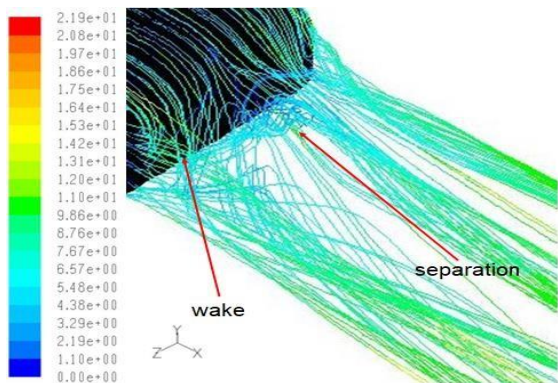
(b)   With blowing active control, UBL1/U0=0.03.
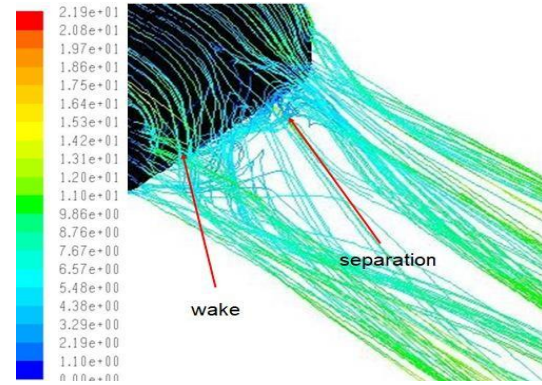
(c)   With blowing active control, UBL2/U0=0.06.
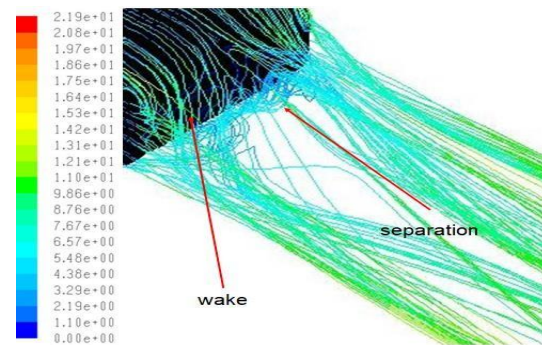
(d)   With blowing active control, UBL3/U0=0.09.

Figure 6. Flow field.

B. Pressure Distribution

Table II shows compares the minimum pressure coefficient for the model with and without blowing at the velocity ratios of $U_{BL1}/U_0=0.03$, $U_{BL2}/U_0=0.06$, and $U_{BL3}/U_0=0.09$.

TABLE II. COMPARISON OF THE MINIMUM PRESSURE COEFFICIENT.

z/w	Without control	With blowing active control, U_{BL}/U_0		
		0.03	0.06	0.09
−1/2	−0.4132	−0.2206	−0.2260	−0.1865
−1/4	−0.3769	−0.2147	−0.2143	−0.1865
0	−0.3405	−0.2206	−0.2143	−0.1865
1/4	−0.3405	−0.2206	−0.2143	−0.1865
1/2	−0.4132	−0.2206	−0.2260	−0.1865
Average	−0.3769	−0.2194	−0.2189	−0.1865
Increase (%)	-	41.7788	41.9080	50.5248

The lowest minimum average pressure coefficient of -0.3769 was found in the model without blowing controls. It was achieved at the grid- to-model height ratio y/h=0.83 as shown in Fig. 7(a). This is because the position of y/h=0.83 is the point of onset for the flow separation. These findings are consistent with a theory that the pressure coefficient is lower at the onset point of flow separation [2]. The pressure for grid-to-model width ratios of z/w=-0.5, z/w=-0.25, z/w=0, z/w=0.25, and z/w=0.5 are written as -0.4132, -0.3769, -0.3405, -0.3405, and -0.4132.

These results correlate with the flow pattern characteristics in Fig. 6(a) which shows that the model without active control is the one with the most apparent wake and vortex formation when compared to other models.

(a). Without control

(b). With blowing active control, $U_{BL1}/U_0=0.03$

(c). With blowing active control, $U_{BL2}/U_0=0.06$

(d). With blowing active control, $U_{BL3}/U_0=0.09$
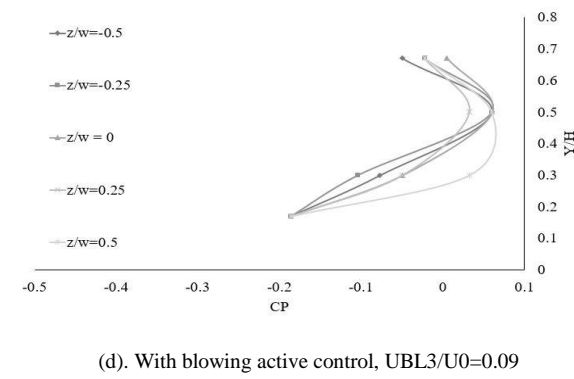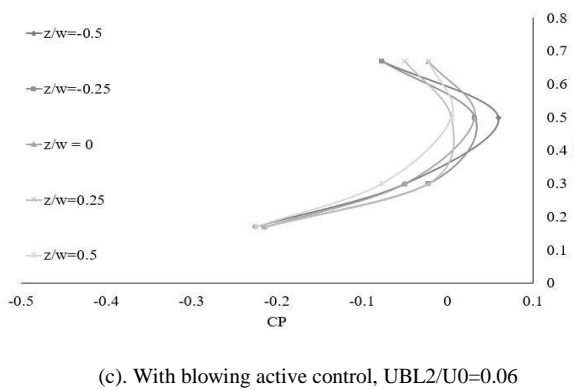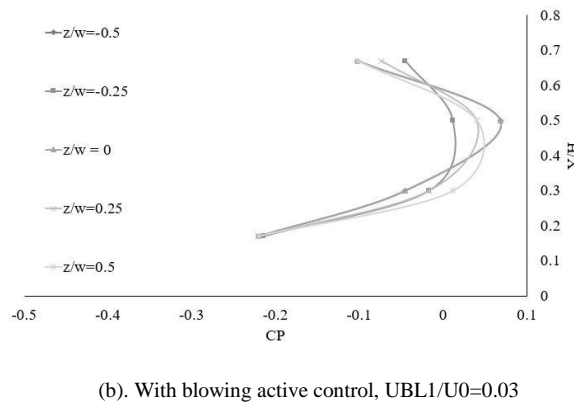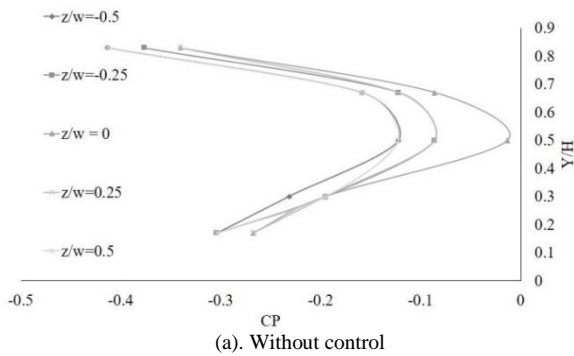
Figure 7. Pressure distribution.

For the model with velocity $U_{BL1}/U_0=0.03$, an increase in the average minimum pressure coefficient is apparent compared to the those in models without blowing. An average minimum pressure coefficient of -0.2194 is obtained at the position y/h=0.17 as shown in Fig. 7(b) with an increase in the percentage of 41.7788%. This is caused by backflow on the lower part of the rear of the test model. Minimum pressure coefficient values at the z/w position are written respectively z/w=-0.5 of -0.2606, z/w= -0.25 of -0.2147, z/w=0 of -0.2206, z/w=0.25 of -0.2206, and z/w=0.5 of -0.2206.

Additionally, the model in the ratio of velocity $U_{BL2}/U_0=0.06$ also indicates an increase in the average minimum pressure coefficient, and this is greater than the one with the velocity ratio of $U_{BL1}/U_0=0.03$. An increase of 41.9080% with an average minimum pressure coefficient of -0.2189 is obtained at position y/h=0.17 as shown in Fig. 7(c), where the value at each position z/w=-0.5, z/w=-0.25, z/w=0, z/w=0.25, and z/w=0.5 are written -0.2260, -0.2143, -0.2143, -0.2143, and -0.2260.

A similar phenomenon also occurred in a model with the velocity ratio of $U_{BL3}/U_0=0.09$, where the application of blowing active control has been capable of increasing the average minimum pressure coefficient despite being higher than the ones with velocity ratios $U_{BL1}/U_0=0.03$ and $U_{BL2}/U_0=0.06$. This increase is equivalent 50.5248% with an average minimum pressure coefficient of -0.1865 obtained at position y/h=0.17 as shown in Fig. 7(d), where the values of pressure coefficients for particular grid-to-model width ratios are stated as follows z/w=-0.5 of -0.1865, z/w=-0.25 of -0.1865, z/w=0 of -0.1865, z/w=0.25 of -0.1865 and z/w=0.5 of -0.1865.

Generally, the application of active control indicates increasing average minimum pressure coefficient, where the model with the ratio of velocity $U_{BL3}/U_0=0.09$ is the model producing the highest increase of the average minimum pressure coefficient. This correlates with the characteristics of the flow shown in Fig. 6(d) where the model at $U_{BL3}/U_0=0.09$ has the smallest wake formation that is tighter and more uniform than that of other models. The research results confirm previous research which also concluded that the application of active control where flow separation formed initially leads to the potential development of the pressure field [20–22].

C. Aerodynamic Drag

The drag coefficient gained through the computational method is shown in Table III. The highest value of 1.845 is found in the model without active control. Meanwhile, models with the active control in various ratios of blowing velocity to upstream velocity shows a decrease in drag coefficients. The drag coefficient is written $U_{BL1}/U_0=0.03$ of 1.636, $U_{BL2}/U_0=0.06$ of 1.628, and $U_{BL3}/U_0=0.09$ of 1.620.

TABLE III. COMPUTATIONAL METHOD DRAG COEFFICIENT.

C_d			
Without control	$U_{BL1}/U_0=$ 0.03	$U_{BL2}/U_0=$ 0.06	$U_{BL3}/U_0=$ 0.09
1.845	1.636	1.628	1.620

In the experimental approach, the highest drag coefficient value of 1.763 was also achieved in the model without active control, as shown in Table IV. Models with active controls on respective ratios of blowing velocity to the upstream velocity show decreases of drag coefficient, stated as follows $U_{BL1}/U_0=0.03$ at 1.563, for $U_{BL2}/U_0=0.06$ at 1.561, and for $U_{BL3}/U_0=0.09$ at 1.559.

TABLE IV. EXPERIMENTAL METHOD DRAG COEFFICIENT.

C_d			
Without control	$U_{BL1}/U_0=$ 0.03	$U_{BL2}/U_0=$ 0.06	$U_{BL3}/U_0=$ 0.09
1.763	1.563	1.561	1.559

Table V compares the drag coefficient of each model, both computationally and experimentally. The model without blowing controls recorded the highest drag coefficient through both computational and experimental methods. It had a difference of 4.434% in drag coefficients, which correlates to the wake structure and the average minimum pressure coefficient. The absence of active control creates the apparent wake, vortex, and re-circulation zone formation, as shown in Fig. 6(a). In contrast, the model with the lowest average minimum pressure coefficient is shown in Table II.

Table V shows that the following ratio of $U_{BL1}/U_0=0.03$, with the application of blowing active control, gives optimum results through computational and experimental methods. The reduction of each method was written 11.328% and 11.321%, respectively. The reduction for the velocity ratio $U_{BL2}/U_0=0.06$, is written as 11.741% for computation and 11.431% for experiments. For the velocity ratio of $U_{BL3}/U_0=0.09$, the reduction are written as 12.187% for the computational method and 11.556% for the experimental one.

Overall, the application of blowing active control positively reduces aerodynamic drag, as shown in Table V, where the model at $U_{BL3}/U_0=0.09$ is the model with the highest aerodynamic drag reduction. This correlates with the flow pattern characteristics shown in Fig. 6(d), and the average minimum pressure coefficient value in Table II, where the model at $U_{BL3}/U_0=0.09$. The model with the smallest wake formation shows tighter and more uniform flow lines. The results are in similar fashion to that of Harinaldi et al., which proved active controls could reduce aerodynamic drag [15].

TABLE V. COMPARISON OF DRAG COEFFICIENTS.

Method	Without control	$Ubl_1/U=0.03$	Reduction (%)	$Ubl_2/U_0=0.06$	Reduction (%)	$Ubl_3/U_0=0.09$	Reduction (%)
Computational	1.845	1.636	11.328	1.628	11.741	1.620	12.187
Experimental	1.763	1.563	11.321	1.561	11.431	1.559	11.556
Difference (%)	4.434	4.428	-	4.099	-	3.747	-

IV. CONCLUSIONS

The application of blowing active control positively affects the flow pattern characteristics, showing delays in the flow separation process. A considerable reduction in wake formation was obtained in the model with the velocity ratio of $U_{BL3}/U_0=0.09$.

The application of blowing active control also positively increases the minimum pressure coefficients for all blowing velocities. The model with the velocity ratio of $U_{BL3}/U_0=0.09$ has the highest increase in minimum pressure coefficient of 50.5248%.

The positive effects are also shown in the form of reduced aerodynamic drag coefficient both computationally and experimentally. The highest reduction was obtained in the model with the velocity ratio of $U_{BL3}/U_0=0.09$, 12.187% and 11.556% for computational and experimental methods, respectively.

CONFLICT OF INTEREST

The authors declare no conflict of interest.

AUTHOR CONTRIBUTIONS

Dr. R. Tarakka, is the lead and corresponding author, who organized research planning and promotion. Dr. N. Salam, Dr. A.A. Mochtar, and Mr. W. Rauf, conducted the research. Mr. M. Ihsan wrote the manuscript. All authors approved the final version.

FUNDING

REFERENCES

[1] R. Tarakka, N. Salam, J. Jalaluddin, and M. Ihsan, "Effect of blowing flow control and front geometry towards the reduction of aerodynamic drag on vehicle models," *FME Transactions*, vol. 47, no. 3, pp. 552–559, 2019, DOI: 10.5937/fmet1903552T.

[2] J. Anderson, *Fundamental of Aerodynamics*, 6th ed. Mc Graw Hill, 2017.

[3] P. Kundu, I. Cohen, and D. Dowling, *Fluid Mechanics - 6th Edition*, 6th ed. Academic Press, 2015. Accessed: Nov. 09, 2021.

[Online]. Available: https://www.elsevier.com/books/fluid-mechanics/kundu/978-0-12-405935-1

[4] S. M. R. Hassan, T. Islam, M. Ali, and Md. Q. Islam, "Numerical study on aerodynamic drag reduction of racing cars," *Procedia Engineering*, vol. 90, pp. 308–313, Jan. 2014, DOI: 10.1016/j.proeng.2014.11.854.

[5] M. Bellman, R. Agarwal, J. Naber, and L. Chusak, "Reducing energy consumption of ground vehicles by active flow control," Dec. 2010, pp. 785–793. DOI: 10.1115/ES2010-90363.

[6] P. Gopal and T. Senthilkumar, "Influence of wake characteristics of a representative car model by delaying boundary layer separation," *Journal of Applied Science and Engineering*, vol. 16, no. 4, pp. 363–374, 2013,DOI: 10.6180/jase.2013.16.4.04.

[7] T. Heinemann, M. Springer, H. Lienhart, S. Kniesburges, C. Othmer, and S. Becker, "Active flow control on a 1:4 car model," *Exp Fluids*, vol. 55, no. 5, p. 1738, May 2014, DOI: 10.1007/s00348-014-1738-0.

[8] T. B. Hilleman, "Vehicle drag reduction with air scoop vortex impeller and trailing edge surface texture treatment," US7192077B1, Mar. 20, 2007 Accessed: Nov. 09, 2021. [Online]. Available: https://patents.google.com/patent/US7192077B1/e n

[9] M. Jahanmiri, "Experimental investigation of drag reduction on Ahmed car model using a combination of active flow control methods," *IJE*, vol. 24, no. 4, pp. 403–410, 2011, DOI: 10.5829/idosi.ije.2011.24.04a.09.

[10] C. H. Bruneau, E. Creusé, D. Depeyras, P. Gilliéron, and I. Mortazavi, "Coupling active and passive techniques to control the flow past the square back Ahmed body," *Computers and Fluids*, vol. 38, no. 10, p. 1875, 2010, DOI: 10.1016/j.compfluid.2010.06.019.

[11] R. Mestiri, A. Ahmed-Bensoltane, L. Keirsbulck, F. Aloui, and L. Labraga, "Active flow control at the rear end of a generic car model using steady blowing," *Journal of Applied Fluid Mechanics*, vol. 7, pp. 565–571, Oct. 2014.

[12] A. Ferraris, H. de C. Pinheiro, A. G. Airale, M. Carello, and D. B. Polato, "City car drag reduction by means of flow control devices," *SAE International*, Warrendale, PA, SAE Technical Paper 2020-36–0080, Mar. 2021. doi: 10.4271/2020-36-0080.

[13] H. Tebbiche and M. S. Boutoudj, "Active flow control by micro-blowing and effects on aerodynamic performances. Ahmed body and NACA 0015 airfoil," *FMR*, vol. 48, no. 2, 2021, DOI: 10.1615/InterJFluidMechRes.2021036842.

[14] J. J. Cerutti, C. Sardu, G. Cafiero, and G. Iuso, "Active flow control on a square-back road vehicle," *Fluids*, vol. 5, no. 2, Art. no. 2, June 2020, DOI: 10.3390/fluids5020055.

[15] Harinaldi, R. Budiarso, Tarakka, and S. P. Simanungkalit, "Computational analysis of active flow control to reduce aerodynamics drag on a van model," *International Journal of Mechanical & Mechatronics Engineering*, vol. 11, no. 03, pp. 24–30, 2011.

[16] M. N. Sudin, M. A. Abdullah, S. A. Shamsuddin, F. R. Ramli, and M. Mohd, "Review of research on vehicles aerodynamic drag reduction methods," *International Journal of Mechanical & Mechatronics Engineering IJMME-IJENS*, vol. 14, no. 2, pp. 35–47, 2014.

[17] B. R. Munson, D. F. Young, and T. H. Okiishi, *Fundamentals of Fluid Mechanics*, 4th ed. John Wiley & Sons Inc, 2002.

[18] Y. A. Çengel and J. M. Cimbala, *Fluid Mechanics: Fundamentals and Applications*. McGraw-Hill Education, 2018.

[19] M. Onorato, A. F. Costelli, and A. Garrone, "Drag measurement through wake analysis," Feb. 1984, p. 840302. DOI: 10.4271/840302.

[20] W. Rauf, R. Tarakka, Jalaluddin, and M. Ihsan, "Effect of flow separation control with suction velocity variation: study of flow characteristics, pressure coefficient, and drag coefficient," *Universal Journal of Mechanical Engineering*, vol. 8, no. 3, pp. 142–151, May 2020, DOI: 10.13189/ujme.2020.080302.

[21] S. Krajnović and J. Fernandes, "Numerical simulation of the flow around a simplified vehicle model with active flow control," *International Journal of Heat and Fluid Flow*, vol. 32, no. 1, pp. 192–200, Feb. 2011, DOI: 10.1016/j.ijheatfluidflow.2010.06.007.

[22] R. Tarakka, Jalaluddin, B. Mire, and M. N. Umar, "Effect of turbulence model in computational analysis of active flow control on aerodynamic drag of bluff body van model," *International Journal of Applied Engineering Research*, vol. 10, no. 1, pp. 207–219, 2015.

Rustan Tarakka – is an Assopciate Professor in the Department of Mechanical Engineering, Faculty of Engineering, Hasanuddin University, Makassar, Indonesia. He holds a doctoral degree from University of Indonesia, Jakarta, Indonesia. His research areas are on fluid dynamics and computational fluid dynamics.

Nasaruddin Salam – is a Professor and the Chairman of Fuild Mechanics Laboratory in Department of Mechanical Engineering, Faculty of Engineering, Hasanuddin University Makassar Indonesia. He holds a doctoral degree from Brawijaya University, Malang Indonesia. His research fields include fluid dynamics.

Andi Amijoyo Mochtar –obtained a Doctor of Engineering in Mechanical Engineering in 2016 from Ehime University Japan. He is an Senior Lecturer of Mechanical Engineering of Hasanuddin University, Makassar, Indonesia..

Wawan Rauf – obtained a Master of Engineering in Mechanical Engineering in 2020 from Hasanuddin University. His research areas are on fluid dynamics and computational fluid dynamics.

Muhammad Ihsan –works for LLDIKTI 9 Sulawesi at Sekolah Tinggi Teknik Baramuli. He holds masters degrees in transport engineering from Asian Institute of Technology, Bangkok, Thailand and Universitas Gajah Mada, Yogyakarta, Indonesia.